Icarus 243 (2014) 274–286

Contents lists available at ScienceDirect

Icarus

journal homepage: www.elsevier.com/locate/icarus

A radiogenic heating evolution model for cosmochemically Earth-like exoplanets

Elizabeth A. Frank [a,*], Bradley S. Meyer [b], Stephen J. Mojzsis [a,c,d,*]

[a] Department of Geological Sciences, NASA Lunar Science Institute, Center for Lunar Origin and Evolution (CLOE), University of Colorado, 2200 Colorado Avenue, UCB 399, Boulder, CO 80309-0399, USA
[b] Department of Physics and Astronomy, Clemson University, Clemson, SC, 29634-0978, USA
[c] Laboratoire de Géologie de Lyon, École Normale Supérieure de Lyon, Université Claude Bernard Lyon 1, CNRS UMR 5276, 2 rue Raphaël Dubois, 69622 Villeurbanne, France
[d] Hungarian Academy of Sciences, Institute for Geological and Geochemical Research, 45 Budaörsi ut, H-1112 Budapest, Hungary

ARTICLE INFO

Article history:
Received 11 August 2013
Revised 12 August 2014
Accepted 19 August 2014
Available online 27 August 2014

Keywords:
Extra-solar planets
Terrestrial planets
Thermal histories
Abundance, interiors
Cosmochemistry

ABSTRACT

Discoveries of rocky worlds around other stars have inspired diverse geophysical models of their plausible structures and tectonic regimes. Severe limitations of observable properties require many inexact assumptions about key geophysical characteristics of these planets. We present the output of an analytical galactic chemical evolution (GCE) model that quantitatively constrains one of those key properties: radiogenic heating. Earth's radiogenic heat generation has evolved since its formation, and the same will apply to exoplanets. We have fit simulations of the chemical evolution of the interstellar medium in the solar annulus to the chemistry of our Solar System at the time of its formation and then applied the carbonaceous chondrite/Earth's mantle ratio to determine the chemical composition of what we term "cosmochemically Earth-like" exoplanets. Through this approach, predictions of exoplanet radiogenic heat productions as a function of age have been derived. The results show that the later a planet forms in galactic history, the less radiogenic heat it begins with; however, due to radioactive decay, today, old planets have lower heat outputs per unit mass than newly formed worlds. The long half-life of ^{232}Th allows it to continue providing a small amount of heat in even the most ancient planets, while ^{40}K dominates heating in young worlds. Through constraining the age-dependent heat production in exoplanets, we can infer that younger, hotter rocky planets are more likely to be geologically active and therefore able to sustain the crustal recycling (e.g. plate tectonics) that may be a requirement for long-term biosphere habitability. In the search for Earth-like planets, the focus should be made on stars within a billion years or so of the Sun's age.

1. Introduction

Since the first extrasolar planet orbiting a main-sequence star was verified in 1995 (Mayor and Queloz, 1995), scores more have been discovered, with >1500 confirmed, >3800 considered candidates, and more being added to the roster every day (http://planetquest.jpl.nasa.gov). The *CoRoT* (*COnvection, ROtation, and planetary Transits*) and *Kepler* telescopes have spearheaded the current era of exoplanet discovery. The primary goal of *CoRoT* is to discover exoplanets with short orbital periods, whereas that of *Kepler* was to find rocky Earth-mass worlds in their star's habitable zone; thus far, the suite of finds runs the gamut from super-Jupiters (e.g. Johnson et al., 2009) to sub-Mercuries (Barclay et al., 2013). Given that *CoRoT* and *Kepler* can directly measure little more than mass and orbital distance, inferring the atmospheric and geophysical regimes of exoplanets requires modeling, which itself necessitates extrapolations and inferences based on knowledge of our own Solar System. Rocky (composed of silicate and metal, also called "terrestrial") exoplanets in particular have received attention for their potential to be geologically active and thus potentially habitable to alien biomes. In the past several years, there has been a flurry of reports attempting to model the interiors of rocky exoplanets, their thermal histories, and the plausibility of present geological activity (e.g. Foley et al., 2012; Fortney et al., 2007; O'Neill, 2012; Papuc and Davies, 2008; Seager et al., 2007; Valencia and O'Connell, 2009; Valencia et al., 2006, 2007). A focus of these modeling efforts has been to determine the tectonic

* Corresponding authors. Address: Department of Geological Sciences, NASA Lunar Science Institute, Center for Lunar Origin and Evolution (CLOE), University of Colorado, 2200 Colorado Avenue, UCB 399, Boulder, CO 80309-0399, USA (S.J. Mojzsis). Fax: +1 303 492 2606.
E-mail addresses: elizabeth.frank@colorado.edu (E.A. Frank), mojzsis@colorado.edu (S.J. Mojzsis).

http://dx.doi.org/10.1016/j.icarus.2014.08.031
0019-1035/

regimes of the so-called "super-Earths" (1–10 $M_{\oplus}$; Valencia et al., 2006), and in particular, whether these worlds are capable of sustaining plate tectonics.

The geophysical state of a super-Earth or any rocky planet is dictated in part by processes that occur long before its Solar System coalesced. The thermal regime of a planetary mantle, which on Earth manifests itself via plume activity and plate tectonics, is set largely by the long-lived, heat-producing radionuclides that were created during nucleosynthesis and injected into the interstellar medium from which all stars and their planetary systems form. The most important of these isotopes, ^{40}K, ^{232}Th, ^{235}U, and ^{238}U, contribute significantly to Earth's modern heat budget, complemented by lingering heat from accretion and differentiation (e.g. Richter, 1988).[1] Estimates of the Urey ratio, or the fraction of Earth's surface heat loss derived from radiogenic heating, range between 0.21 and 0.74 (Lenardic et al., 2011 and references therein). Despite their slow decay (^{40}K, $\tau_{1/2}$ = 1.25 Gyr; ^{232}Th, $\tau_{1/2}$ = 14.0 Gyr; ^{235}U, $\tau_{1/2}$ = 0.704 Gyr; and ^{238}U, $\tau_{1/2}$ = 4.47 Gyr), the concentrations of the long-lived isotopes in Earth's mantle have declined significantly over geologic time. For example, although ^{235}U was 88 times more abundant at the time of Solar System formation (t_{ss} = 4.568 Ga; Amelin et al., 2002; Bouvier and Wadhwa, 2010) than it is now, it became effectively extinct in Earth's mantle after less than about 3 Gyr. This has left the other three isotopes to produce the radiogenic heat that helps sustain Earth's present geological activity. With a half-life comparable to the age of the Universe, ^{232}Th has lost a mere 20% of its original abundance since t_{ss}, while ^{40}K has lost ~90%. When Earth reaches an age of ca. 10 Gyr, its radiogenic heat production will be ~15% of what it was at t_{ss}. At that time, ^{40}K will no longer be a heat contributor and ^{232}Th will continue to dominate heat production as it does today. In as soon as 900 Myr from now, there may no longer be enough heat in the mantle to sustain mobile-lid convection, and plate tectonics will shut down (Sleep, 2007).

Despite how significantly Earth's own heat production has changed with time, exoplanet modelers assume modern Earth, primordial Earth, or chondritic values for the concentrations of the important heat-producing nuclides. This is due to the challenge of having no direct data on the chemistry of rocky exoplanets, and thus, one is forced to make assumptions based on our Solar System with the understanding that it may not be representative of the hundreds of billions of others in the Galaxy. Furthermore, most exoplanet models inaccurately assume a heat production rate at steady-state rather than one that declines over time. This is especially important to recognize because while the age of a planet plays a pivotal role in the relative heat contributions of the relevant isotopes, it is equally important to consider their initial concentrations (cf. Gonzalez et al., 2001; Kite et al., 2009) since the ability of a planet to sustain plate tectonics changes with its initial and evolving thermal profile, which in turn affects its resulting surface convective regime (Noack and Breuer, in press). To constrain the initial radiogenic heat production of a planet, it is necessary to turn to galactic chemical evolution (GCE) models that predict the chemical composition of the gas in the galactic disk—and therefore the solar systems and planets that form from it—over the Galaxy's history. By coupling the chemical evolution of the Galaxy with that of solar systems and their planets, we have made first-order predictions of the ^{40}K, ^{232}Th, ^{235}U, and ^{238}U concentrations in rocky exoplanets within the solar annulus (an annular region centered on the Sun's orbit in the Galaxy), and in doing so, have generated radiogenic heating estimates for these exoplanets as a function of their age.

[1] The important heat-producing short-lived nuclides ^{26}Al ($\tau_{1/2} = 7.17 \times 10^5$ y) and ^{60}Fe ($\tau_{1/2} = 2.6 \times 10^6$ y) become effectively extinct about 3 Myr after they form and thereafter cease to contribute to heat production.

2. Galactic chemical evolution

Astrophysicists have long been faced with the challenge of trying to encapsulate the chemical evolution of the Galaxy into a single cohesive narrative (Burbidge et al., 1957). To tackle this problem, GCE models were formulated to address how the bulk chemistry of the Galaxy changes in both time and space as old stars perish and new generations arise (Matteucci, 2003). They quantitatively describe how the Galaxy evolves chemically as gas collapses into stars, stars generate "metals" (in the context of astrophysics, elements heavier than H and He) via nucleosynthesis, and the new elements are released back into the gas at the end of a star's lifetime. All GCE models share four common components: (i) boundary conditions, such as the Galaxy's initial composition and whether it is an open or closed system; (ii) stellar yields of heavy nuclides produced by nucleosynthesis; (iii) a star formation rate (SFR) and the initial mass function (IMF), which describes the distribution of initial masses for a stellar population; and (iv) gas inflows and outflows to the galactic system (Pagel, 1997). Quantitative constraints on GCE models include solar and meteorite compositions derived from observation and direct measurements of solar wind, the solar photosphere, the abundance ratios of the isotopes in primitive meteorites, the metallicity of G-dwarf stars, and galactic abundance gradients (Nittler and Dauphas, 2006). The resulting output is strongly model-dependent given the uncertainties inherent in each component. Operating as they do over colossal length scales for billions of years, nucleosynthetic processes enrich the interstellar medium (ISM) with heavy elements that accumulate and mix into the mass of material that supplies star-forming regions (Cowan and Sneden, 2006).

The effectively instantaneous appearance of heavy elements was due to production in the first generation of massive stars that lived on the order of 10^6 years after the Galaxy formed (Bromm and Larson, 2004), a period of time that was brief compared to the lifetime of the Galaxy. Indeed, a recent discovery of a galaxy that formed 700 Myr after the Big Bang and has a SFR > 100 times our Galaxy's provides evidence for the rapid heavy element enrichment of galaxies following their formation (Finkelstein et al., 2013). Due to their intrinsic instability as radioactive isotopes, the long-lived, heat-producing nuclides enter the decay process as soon as they are generated. Although it is unclear how the rate of supernova explosions has changed over time, early Solar System abundances of the actinides are approximately that expected for near-uniform production since the Galaxy formed (Reeves, 1991; Wasserburg et al., 1996).

The predictions set forth in GCE models have important implications for bulk chemical properties of planets, and so the models must account for the different processes by which elements are generated. The actinides U and Th are produced in the rapid-process ("r-process") nucleosynthesis, in which seed nuclei at the Fe peak experience a series of neutron captures that occur rapidly relative to the rate of β-decay if the nucleus is unstable (e.g. Cowan et al., 1991). Because of the neutron densities required for the r-process to occur, it was originally suggested that this happens in the neutron-dense areas around neutron stars produced in supernovae (Burbidge et al., 1957). Other sites have been proposed such as binary neutron star or black hole mergers, quick low-mass supernova explosions, accretion-induced collapse models, and bubbles or jets produced during supernova explosions (Sneden et al., 2008). In contrast, ^{40}K is created both during oxygen burning when lighter elements fuse in the cores of massive stars and s-process (slow-process) nucleosynthesis, and it has a different galactic accumulation history than the r-process nuclides (Clayton, 2003; Zhang et al., 2006). These different histories must be taken into account in GCE models.

3. Model

The initial chemistry of a solar system will reflect the composition of the molecular cloud from which it formed at a given time in galactic history. As such, by modeling the chemical evolution of the ISM, we can model the chemical evolution of stars and their Solar Systems. G-dwarf stars (~0.9–1.1 $M_\odot$) are not sites of heavy-element nucleosynthesis but have envelopes that match the composition of their source ISM (Nittler and Dauphas, 2006). Inverting this relationship, the composition of the Sun can be used as a fit to the chemistry of the gas from which it formed at Solar System formation. Ignoring Li, Be, B, noble gases, and other volatile elements, we can make the implicit assumption that like our own Solar System, the composition of bulk solar system materials (i.e. carbonaceous chondrites) reflects that of its star (e.g. Anders and Grevesse, 1989; Lodders, 2003). From this it follows that the bulk silicate material of an extrasolar system should have comparable abundances of the long-lived, heat-producing nuclides to its star as a function of age. This is where GCE models are required.

3.1. An analytical approach

Given that the scale and complexity of what they describe is vast, GCE models are notoriously difficult to construct. Although there are a number of detailed numerical models (Matteucci, 2003), they must take into account a myriad of processes to describe galactic chemistry. To simplify the approach but maintain the required rigor, Clayton (1985) presented a model that parameterizes galactic infall in such a way that it provides analytical solutions for disk gas mass, total star mass, and metallicity. The Clayton model is a mathematical approximation for those GCE models that do simulate the physical processes at hand. This approach is advantageous because the parameterization allows for adjustments to the overarching equations in order to fit trends to astronomical observations.

The Clayton model incorporates several simplifying assumptions to streamline the analysis. This includes the instantaneous recycling approximation (IRA), which states that stellar lifetimes are negligible relative to the timescale of gas consumption, and the instantaneous mixing approximation (IMA), which assumes that stellar ejecta are mixed instantaneously in the ISM. Together, these assumptions imply that short-lived massive stars, which have lifetimes on the order of Myr, live, die, and eject their material back into the ISM on timescales so brief relative to the age of the Galaxy that their lifecycles and contributions are effectively instantaneous. Additionally, the initial mass function (IMF), which sets the population distribution of stars, is time-dependent, and the star formation rate (SFR) is set to depend linearly on the gas mass (i.e. the SFR is proportional to the gas mass). While these simplifying principles make the model less complex than other GCE models, the arbitrary parameters allow for this mathematical model to be satisfactorily adjusted to match astronomical observations.

3.2. Assumptions

In addition to the assumptions described above that are inherent to the Clayton model, we incorporate several of our own to be conservative in the application of and implications for predictions of the geochemistry of exoplanets:

1. Supernova-driven mixing in the interstellar medium in the Sun's neighborhood occurs on a ~100 Myr timescale (de Avillez and Mac Low, 2002). In addition, we expect mixing from shear forces in the differentially rotating galactic disk. The timescale for this mixing is likely to be of the same order of magnitude as the galactic rotation period in the Sun's neighborhood, ~250 Myr (e.g. Mihalas and Binney, 1981). Thus, within the solar annulus, short-lived nuclides may experience inhomogeneous mixing on the timescale of their half-lives, but the half-lives of the long-lived radionuclides of interest are sufficiently long that this is not a concern (Huss et al., 2009).
   In stars in the vicinity of the Sun, Fe shows a radial chemical gradient of roughly −0.065 dex per kiloparsec (Boeche et al., 2013), corresponding to a ~14% drop in Fe abundance relative to H for every 1 kiloparsec. This suggests radial mixing occurs on a longer timescale than azimuthal mixing. For this reason, we restrict our GCE model to the volume of the solar annulus, which we assign to be several hundred parsecs in width, over which radial distance abundances are fairly constant.
2. The equations are fit to the element and isotope mass fractions reported by Anders and Grevesse (1989) for the Solar System at the time of its formation. Thus, linking this to Assumption (1), the composition of all the gas in the solar annulus matches that of our Solar System at its formation ca. 4.568 Ga.
3. The Galaxy is 12.5 ± 0.9 Gyr old (Dauphas, 2005). This estimate is based on the U/Th ratio in meteorites and comparisons to observations of low-mass stars in the galactic halo, thereby connecting cosmochemical data to astronomical observations.
4. There is no contribution to the metals from infalling primordial gas that builds up the galactic disk, i.e. $z_f = 0$, where z_f is the mass fraction of a species in this infalling gas (Clayton, 1985). This assumption is necessary because there is little information about what those fractions are. Furthermore, the fractional contribution of radioactive species will not be constant with time due to their decay, adding further uncertainty to any assumptions. Here, the infalling gas is assumed to be metal-free and thus composed exclusively of H and He.
5. The current mass fraction of gas in the solar annulus is 0.2, with the remainder locked in stars, a value consistent with the range 0.15–0.25 estimated from observations of the surface densities of gas, stars, and stellar remnants in the solar neighborhood (Boissier and Prantzos, 1999 and references therein).
6. The predictions for exoplanets only apply to what we term "cosmochemically Earth-like" worlds around other stars, which are those that hypothetically possess the same elemental and isotopic ratios that Earth has relative to carbonaceous chondrites. (A more detailed description of this assumption can be found in Section 4.3).

3.3. Relevant equations

The Clayton model is designed to track how the chemistry of gas in the galactic disk and that of a particular species (isotope, element, or molecule) changes as a function of time. Gas in the disk initially builds up by infall of metal-poor primordial matter and is subsequently consumed by stars, the rate of which changes over time and is described by the star formation rate. Some fraction of mass in stars is ejected during supernova explosions and returned to the ISM, but as the Galaxy chemically evolves, gas becomes increasingly locked in stars. The mass fraction evolution of a species i in the disk process can be qualitatively described by

$$\frac{d(M_G \cdot Z_i)}{dt} = -(\text{loss to stars}) + (\text{gain from stars}) - (\text{loss from radioactive decay}), \quad (1)$$

where M_G is the gas mass of the disk, Z_i is the mass fraction of a species in the gas, and t is time since Galaxy formation. Fig. 1 is a schematic of these linked processes, the net chemical effect of which is metal enrichment in the ISM from the metal-free infalling gas. The

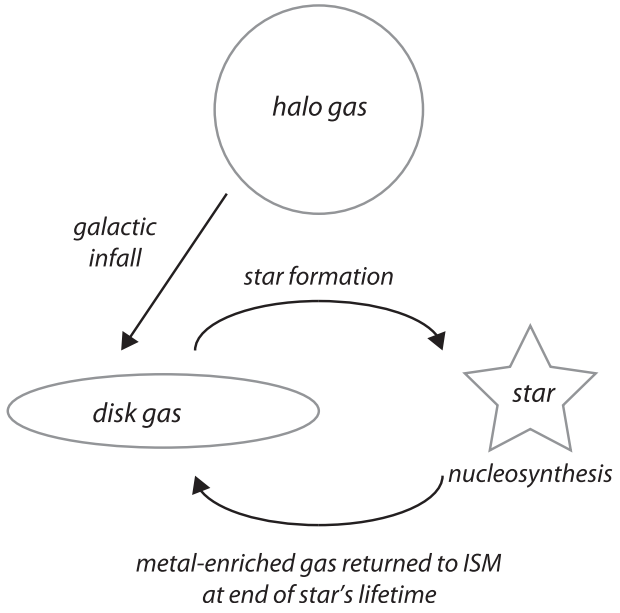

Fig. 1. Schematic showing the flow of mass through the galactic disk.

linear relationship between the SFR and gas mass is described by the equation

$$\frac{dM_G}{dt} = -\omega M_G + f(t), \tag{2}$$

where ω is the rate of mass consumption from star formation (constant for all species) and $f(t)$ is the infall rate of metal-poor primordial gas to the disk (in our case, only the solar annulus). Finally, the standard parameterized model of Clayton (1985) quantifying galactic infall's relationship to gas mass (for our purposes, in the solar annulus) is given by:

$$\frac{f(t)}{M_G(t)} = \frac{k}{t+\Delta}, \tag{3}$$

where k is a positive integer (0, 1, 2, 3) and Δ is a parameter with units of time. The parameterized equation for $M_G(t)$ is

$$M_G(t) = M_G(0)\left(\frac{t+\Delta}{\Delta}\right)^k e^{-\omega t}, \tag{4}$$

where $M_G(0)$ is the initial mass of the solar annulus at the time of formation.

These equations lay the groundwork for computing the evolving mass fractions of a particular species in the gas. Most of the species considered here are only primary, meaning that they can form in the cores of massive stars composed solely of H and He and do not require seed nuclei. Tinsley (1979) recognized that the galactic chemical evolution of ^{56}Fe received an additional primary boost from Type Ia supernovae, which caused a growing Fe abundance relative to other primary elements after a few Gyr in galactic history. Type Ia supernovae are the thermonuclear explosions of white dwarf stars, and their onset is delayed by the time required to evolve the white dwarf progenitor (Matteucci and Greggio, 1986). In contrast, the nuclide ^{40}K has both primary and secondary components. Secondary species form from seed nuclei and thus require a previous generation of stars to live and die before adding their metals to the ISM. The yield from stellar nucleosynthesis (y_i) for species i is the sum of the primary (α_i) and secondary (β_i) yield terms, where the total yield of all primary species (y_p) is used to calculate the secondary contribution:

$$y_i = \alpha_i + \beta_i y_p. \tag{5}$$

Yield is expressed as the mass of species i ejected from a generation of stars per unit of mass locked up in stellar remnants. When a particular species is purely primary, $\beta_i = 0$ and $y_i = \alpha_i$.

From here the yield is used to calculate the evolution of a species' mass fraction (Z_i) in gas over the age of the Galaxy:

$$\frac{dZ_i}{dt} = y_i\omega - \lambda_i Z_i - (Z_i - Z_{f,i})\frac{f(t)}{M_G(t)}, \tag{6}$$

where λ_i is the decay constant in the case of a radioactive species ($\lambda_i = 0$ for a stable species) and $Z_{f,i}$ is the mass fraction contribution of a species from galactic infall. Because the infalling primordial matter being considered here is metal-free, in our model we assume $Z_{f,i} = 0$. This governing equation leads to individual equations for the mass fraction evolution of stable and unstable species. That for a stable species is described by

$$Z_i = \left(\frac{y_i\omega\Delta}{k+1}\right)\left[\frac{t+\Delta}{\Delta} - \left(\frac{t+\Delta}{\Delta}\right)^{-k}\right]. \tag{7}$$

In contrast, radioactive species are described by

$$Z_i = (y_i\omega - \lambda_i Z_{f,i})e^{-\lambda t}\left(\frac{\Delta}{t+\Delta}\right)^k I_k(t,\lambda_i), \tag{8}$$

where $I_k(t, \lambda_i)$ is an integral that depends on the assumed k. For $k = 1$, this equation is

$$I_1 = \frac{1}{\Delta}\left[e^{\lambda t}\left(\frac{t+\Delta}{\lambda} - \frac{1}{\lambda^2}\right) - \left(\frac{\Delta}{\lambda} - \frac{1}{\lambda^2}\right)\right]. \tag{9}$$

The equations outlined above are the analytical solutions for the Clayton GCE model. A thorough derivation of these equations can be found in Clayton (1985), and details of the code used for the computations is available online as Supplementary File S1.

4. Results

4.1. Gas mass evolution

The evolution of the gas mass in the Clayton model depends on the choice of the parameters k, Δ, and ω. Following standard practice (e.g. Clayton, 1985), we choose $k = 1$ and $\Delta = 0.1$. From the requirement that the fraction of the mass in the solar annulus be ~20% (Boissier and Prantzos, 1999), we then determined ω to be 0.211 Gyr^{-1}. We note that varying Δ has little effect on the resulting value for ω, while the effect of varying k is much larger (Huss et al., 2009).

Fig. 2 shows the evolution of the total mass (relative to the initial mass $M_G(0)$) of the solar annulus, the mass in gas, and the mass in stars as computed from our choice of k, Δ, and ω. The mass of the solar annulus builds up due to infall. Since the infall rate declines with time, the rate of growth of the total mass also declines. The gas mass initially grows, but as the infall rate declines, gas is increasingly locked up into stars. The gas fraction declines and reaches the 20% value observed today.

Our choice of model parameters agrees with two key observations. First, the choice of $k = 1$–2 is consistent with the G dwarf star age-metallicity relationship (e.g. Clayton, 1985). Second, Madau et al. (1998) showed from observations of distant galaxies that the SFR peaked at a redshift of approximately 1.5, which corresponds to a time of ~2–3 Gyr after the Big Bang. The peak in the gas mass (and by the proportionality of this quantity to the SFR) in the SFR is at ~4 Gyr in Fig. 2, but we note that the gas fraction of the Milky Way as a whole is ~0.1–0.15 (e.g. Boissier and Prantzos, 1999). This lower gas fraction would require a larger ω than the one we used, which would push the gas mass peak for the whole Galaxy (not the solar annulus) to earlier times (near

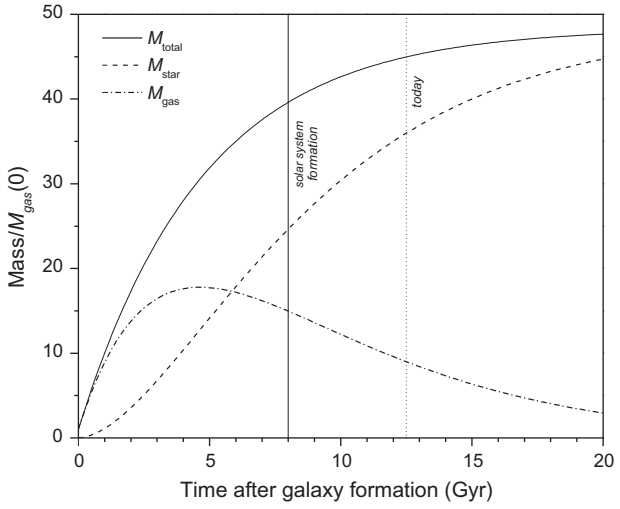

Fig. 2. The evolution of mass in the galactic disk (relative to the initial disk mass). Infall of primordial gas rapidly increases the total mass of the disk but levels off asymptotically. The mass of the gas component peaks early in galactic history, following which disk material becomes increasingly trapped in long-lived stars. The solar neighborhood is currently approximately 20% gas by mass (Boissier and Prantzos, 1999).

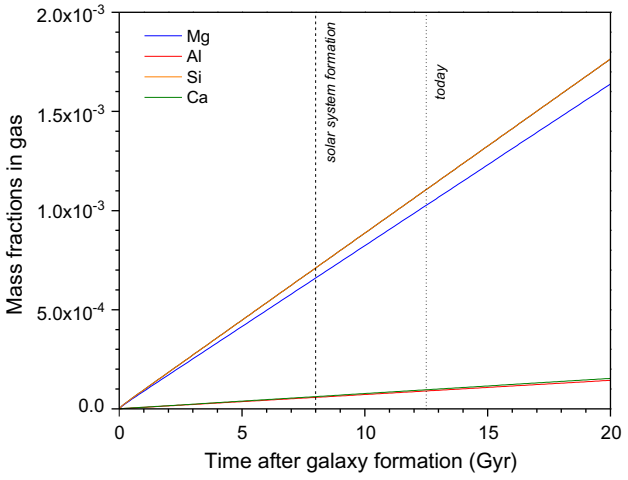

Fig. 3. Mass fractions of several of the major mantle-forming elements. In the analytical Clayton model, these are primary species that experience a constant state of enrichment in the gas since the gas is initially metal-free and have concentrations that are fit to CI values at the time the Solar System formed.

~2–3 Gyr). We thus expect that our choice of parameter values is consistent with observations of star formation at high redshift. We use our choice of k, Δ, and ω throughout the remainder of this work.

4.2. Mass fractions

Output from the Clayton model yields species abundances in terms of mass fractions (Z_i). At $t = 0$ (where t is time after Galaxy formation), the gas starts as being metal-free before being enriched by the nucleosynthesis products of the first generation of massive stars. Because the species mass fractions in the gas of the solar annulus are known for our Solar System from measurements of chondrite meteorites and the solar photosphere, the model is fit to those values at $t = 8$ Gyr. (Since the age of the Solar System is ~4.5 Gyr and the age of the Galaxy is 12.5 Gyr, we assume that the Solar System formed 8 Gyr into galactic history.) For the case of stable, primary-only species, the gas experiences a constant rate of enrichment, as shown in the example of Mg, Al, Si, and Ca in Fig. 3. This is also the case for all species considered here except for ^{56}Fe and ^{40}K.

Iron-56 is a special case due to an additional production source found in Type Ia supernovae, which is the explosive result of a white dwarf (the remnant of a low-mass star that has reached the end of its lifetime and no longer experiences fusion) in a binary system that reaches critical mass from the stripping of material from its companion star, reigniting fusion for a few seconds and burning heavy elements that are immediately ejected (Hillebrandt and Niemeyer, 2000). Because Type Ia supernovae occur at the end of a star's lifetime, their contributions to gas do not begin until the first generation of these low-mass stars has lived and died. This occurs ~1 Gyr after Galaxy formation (Matteucci and Greggio, 1986). At that time, there is an increase in ^{56}Fe production, as shown in Fig. 4A. We model the yield of ^{56}Fe as the sum of two primary terms, α_1 due to massive stars and α_2 due to Type Ia supernovae. Early in Galactic history we take the yield to be α_1, but, as the Galaxy ages, the yield evolves to $\alpha_1 + \alpha_2$. We chose α_1 and α_2 and the timescale for evolution of the total ^{56}Fe from α_1 to $\alpha_1 + \alpha_2$ to reproduce galactic disk oxygen

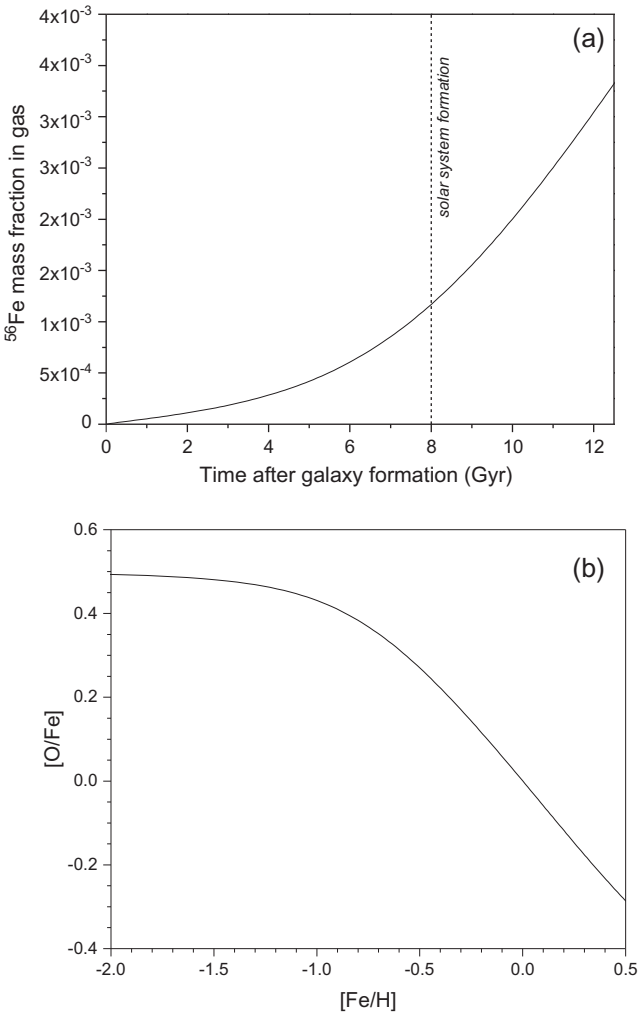

Fig. 4. (A) Mass fraction evolution of Fe in gas. Initially, it is only produced in massive stars, but ~1 Gyr after formation, Type Ia supernovae begin contributing Fe to the gas, boosting its production rate. (B) The evolution of the abundance ratio O to Fe (relative to solar) with evolving Fe to H abundance ratio (also relative to solar) in the disk.

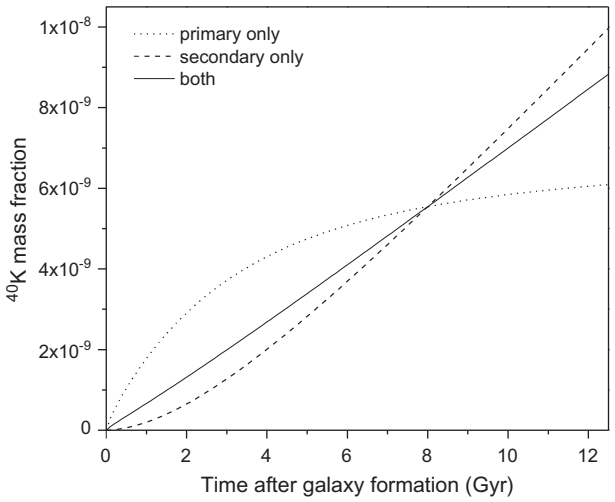

Fig. 5. Mass fraction evolution of ^{40}K in gas. Endmember scenarios for the ^{40}K being only primary or secondary are shown, with a best fit that we selected (solid line) located between the two.

versus iron trends. Fig. 4B shows our resulting [O/Fe] versus [Fe/H][2] curve, which compares favorably with data (e.g. Bensby et al., 2004) and detailed GCE models (e.g. Chiappini et al., 1997).

Potassium-40 is a different case in that it can be produced as both a primary and secondary species. While its abundance in our Solar System at the time of formation is known, the relative proportion of the two contributions is not. Owing to this uncertainty, we model endmember production scenarios in which ^{40}K is only primary or only secondary (Fig. 5). We then take a best fit to the two that incorporates contributions from both primary and secondary sources but later account for the range of plausible resulting concentrations and heat productions on the planetary scale.

4.3. Scaling to planets

Since our model makes predictions for the composition of the ISM from which solar systems form, the species mass fraction output is for bulk solar system material, which for our Solar System is represented by the solar photosphere or CI carbonaceous chondrites minus volatile elements. These figures are not appropriate for direct insertion into geophysical models of rocky exoplanets. When planets form and differentiate, elements fractionate according to their affinities for gas, metal, or silicate species (Goldschmidt, 1954); namely, atmophile ("gas-loving") elements concentrate in atmospheres, lithophile ("rock-loving") elements accumulate into silicate mantles and crusts, and siderophile ("iron-loving") elements descend into cores. Differentiation separates metal and siderophile elements from silicate and lithophile elements as metal descends into the burgeoning core, so from an early stage, the bulk silicate Earth (BSE) experienced fractionation of incompatible elements into crustal components (Caro, 2011 and references therein). To account for fractionation, we scale the bulk Solar System concentration output to Earth-like values by using the ratio of the relevant isotopes between the concentrations of Earth's mantle and CI values.

It is clearly a challenge to make the leap from the scale of bulk solar system chemistry to that of an individual planet. Currently, inferring the composition of a particular exoplanet from that of its star requires many assumptions. To sidestep this issue, we only consider here what we term "cosmochemically Earth-like exoplanets" whose bulk solar system/planet ratios for the species of interest match those of the Earth relative to our Solar System. We justify this approach in several ways:

1. No formation model can currently explain all observed properties of our Solar System. The modeling is challenging: one must reconcile the chemistry, location, and mass of each planet. This remains an active area of research (e.g. Bond et al., 2010) but is currently impossible to perform for exoplanets due to the paucity of information about their planetary systems. With this in mind, we consider only planets that possess species in abundances identical in proportion to that between Earth and CI chondrites.
2. An "Earth-like" exoplanet is commonly defined as one that is close to Earth's size and lies within its star's so-called habitable zone. However, there are many distinct characteristics about Earth than make it what it is, not the least of which is chemistry. With a single example for life in the Universe, we only have Earth on which to base our definition of a habitable planet. Assuming an Earth-scaled chemistry for a planet incorporates the assumption that an Earth-like planet is also chemically Earth-like.
3. Applying such a ratio takes into account any stochastic accretion processes that went to building Earth and evolving it to its current state, such as the Moon-forming Giant Impact (Canup, 2008), Late Veneer (Chou, 1978), planet migration, and Late Heavy Bombardment (Gomes et al., 2005).
4. The chemical compositions of the bulk Solar System (from carbonaceous chondrites and observations of the solar photosphere) and Earth's mantle (from peridotites) are reasonably well constrained and provide hard numbers with which to fit the GCE model.

Quantitatively, we apply this simple formula to the mass fraction output of a particular species to find its abundance in the mantle of a cosmochemically Earth-like exoplanet:

$$\frac{\text{CI chondrite}}{\text{Earth's mantle}} = \frac{\text{modeled bulk solar system}}{\text{predicted exoplanet mantle}} \quad (10)$$

Table 2 shows the canonical chemical abundances used for CI chondrites (Anders and Grevesse, 1989) and Earth's mantle's abundances of major elements (Kargel and Lewis, 1993; McDonough and Sun, 1995) and the relevant radiogenic species (Turcotte and Schubert, 2002).

4.4. Results for Solar Systems at time of formation

After applying the CI/mantle scaling factor to the mass fraction output, we can make predictions for the concentrations of the species in the rocky mantles of cosmochemically Earth-like planets.

4.4.1. Concentrations

Fig. 6 shows the calculated concentrations of ^{40}K, ^{232}Th, ^{235}U, and ^{238}U as a function of the time of formation of generic exoplanets after Galaxy formation. Abundances of those isotopes in Earth's mantle when it formed at t = 8 Gyr are shown for reference. The curves show that the later a planet forms in galactic history, the lower its starting concentrations of the isotopes will be. This is because while the isotopes are being continually produced as the Galaxy ages, they are also simultaneously decaying, whereas the stable species ostensibly are not. As a result, ^{40}K, ^{232}Th, ^{235}U, and ^{238}U are essentially being diluted by the buildup of the stable major mantle-forming elements as the Galaxy ages.

[2] The notation [X/Y] is defined as $[X/Y] = \log_{10}(X/X_{solar}) - \log_{10}(Y/Y_{solar})$. Thus, for example, [Fe/H] = 0 indicates Fe has a solar value.

4.4.2. Heating

While the concentrations of the isotopes are instructive in showing their evolution relative to the stable mantle-forming elements, those concentrations do not directly translate to radiogenic heating. Each isotope has a different specific heat output per unit mass (Table 1). For example, while ^{40}K clearly dominates in concentration, ^{235}U has the highest heat output. Fig. 7 shows the relative heat contributions of each isotope to a planet's mantle at the time of formation. Owing to its short half-life but high heat production, ^{235}U is the most important isotope in heating planets within ~5 Gyr after Galaxy formation. After that, ^{40}K takes over. The dilution effect is particularly apparent in terms of heating: planets that formed immediately after the Galaxy formed would have had more than twice as much initial heating than the Earth did at the time of its formation. The rate of decline in total initial heat production is slowing such that a planet forming today starts with ~5×10^{-12} W kg^{-1} less than Earth when it formed.

Given that radiogenic heating at the time of a planet's formation is one of the parameters that will dictate the planet's tectonic regime and evolution thereof, accounting for the time of a planet's formation and resulting initial heating is crucial. This factor has not been quantitatively accounted for in exoplanet models thus far. To underscore the effect of a planet's time of formation on its thermal evolution, Fig. 8 shows the heat production 4.5 Gyr after formation in planets that formed at t = 0, 4, 8, and 12.5 Gyr into galactic history (where t = 8 Gyr is when Earth formed). Planets that formed soon after Galaxy formation will always have more heat at a particular point in their geologic history than those that formed later. As the isotopes decay, their concentrations will converge as they approach zero, and so heat productions are more similar as planets age. However, the initial concentration helps set a planet's tectonic regime, and so starting with an appropriate initial value is of key importance (Noack and Breuer, in press).

Table 1
Key model parameters.

Constant	Value	Reference
Half-lives (Ga)		
^{40}K	1.25	Turcotte and Schubert (2002)
^{232}Th	14.0	
^{235}U	0.704	
^{238}U	4.47	
Milky Way age (Ga)	12.5	Dauphas (2005)
Solar System age (Ga)	4.56	Amelin et al. (2002) and Bouvier and Wadhwa (2010)
Specific heat production (W/kg isotope)		
^{40}K	2.92×10^{-5}	Turcotte and Schubert (2002)
^{232}Th	2.64×10^{-5}	
^{235}U	5.69×10^{-4}	
^{238}U	9.46×10^{-5}	
Initial mantle concentrations (ppb)		
^{40}K	463.6	Calculated from Turcotte and Schubert (2002)
^{232}Th	155.0	
^{235}U	16.4	
^{238}U	62.4	
Mantle concentrations today (ppb)		
^{40}K	36.9	Turcotte and Schubert (2002)
^{232}Th	124	
^{235}U	0.22	
^{238}U	30.8	

Table 2
Chemical abundances used for our Solar System and the Earth.

	Solar System	Reference	Earth's mantle	Reference	Scaling factor
C	3.07×10^{-3}	1	1.20×10^{-4}	2	0.0391
O	9.62×10^{-3}	1	4.44×10^{-1}	3	46.2
Na	3.34×10^{-5}	1	2.67×10^{-3}	2	80.0
Mg	6.60×10^{-4}	1	2.28×10^{-1}	2	345
Al	5.80×10^{-5}	1	2.35×10^{-2}	2	405
Si	7.11×10^{-4}	1	2.10×10^{-1}	2	295
S	4.18×10^{-4}	1	2.50×10^{-4}	2	0.598
K	3.74×10^{-6}	1	2.40×10^{-4}	2	64.2
Ca	6.20×10^{-5}	1	2.53×10^{-2}	2	408
Ti	2.91×10^{-6}	1	1.21×10^{-3}	2	414
Cr	1.78×10^{-5}	1	2.63×10^{-3}	2	148
Fe	1.17×10^{-3}	1	6.26×10^{-2}	2	53.6
Ni	7.34×10^{-5}	1	1.96×10^{-2}	2	267
SUM	0.0160		1.02		
^{40}K	5.54×10^{-9}	1	4.64×10^{-7}	4	83.6
^{232}Th	2.46×10^{-10}	1	1.55×10^{-7}	4	629
^{235}U	3.41×10^{-11}	1	1.64×10^{-8}	4	483
^{238}U	1.09×10^{-10}	1	6.24×10^{-8}	4	573

References: 1. Anders and Grevesse (1989), 2. McDonough and Sun (1995), 3. Kargel and Lewis (1993) (because no O reported in McDonough and Sun (1995)), 4. Turcotte and Schubert (2002).

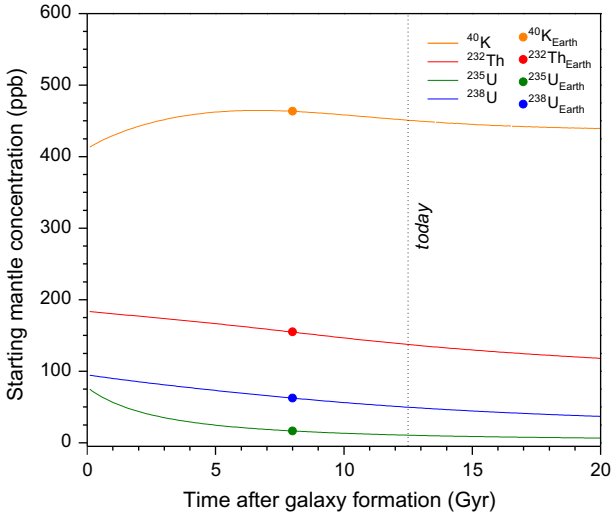

Fig. 6. The initial concentrations of ^{40}K, ^{232}Th, ^{235}U, and ^{238}U in cosmochemically Earth-like mantles as a function of the time at which they formed in galactic history. The dots indicate their concentration in Earth's mantle at the time of its formation.

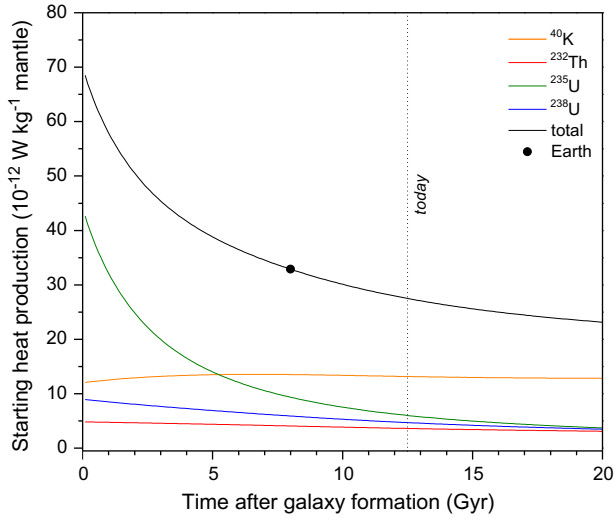

Fig. 7. The initial heat productions of ^{40}K, ^{232}Th, ^{235}U, ^{238}U, and their total in cosmochemically Earth-like exoplanet mantles as a function of their formation time. The black dot indicates Earth's mantle's starting heat production rate.

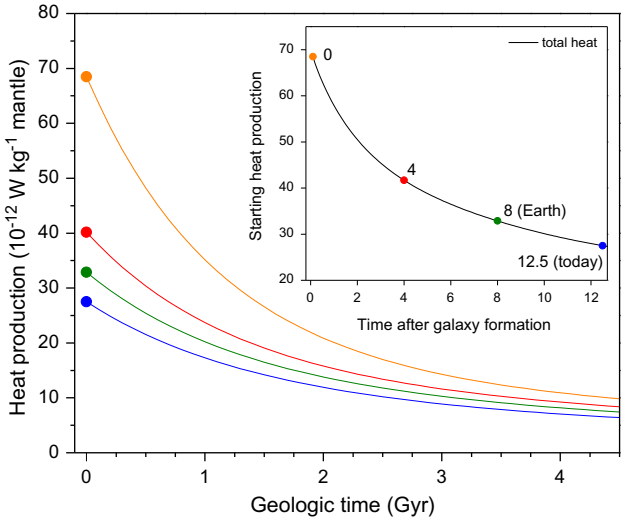

Fig. 8. Heat production rates for the first 4.5 Gyr of geologic history after exoplanets that formed 0, 4, 8, and 12.5 Gyr into galactic history accreted.

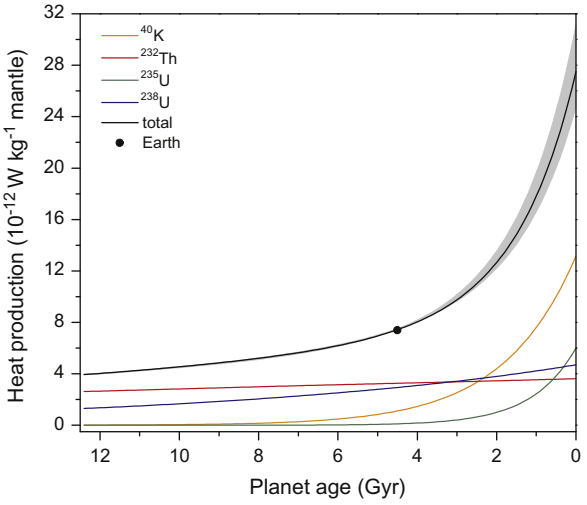

Fig. 10. Current heat production in exoplanets as a function of their age. The gray band shows the range of heat productions of ^{40}K depending on the relative proportions of primary versus secondary contributions.

4.5. Results for Solar Systems today

While the initial heating in a planetary mantle is key to setting the conditions for its tectonic evolution, it is also important to consider its current heat production, as a planet that is too cool cannot sustain plate tectonics, if it ever did so in the first place.

4.5.1. Concentrations

We now consider the current heat production in planets as a function of their age at the present time. To do this, the concentrations of the isotopes are decayed based on how long they have had to decay, i.e. the age of the planet. Again, the age of the Galaxy is assumed to be 12.5 Gyr (Dauphas, 2005). Fig. 9 shows the predicted concentrations of ^{40}K, ^{232}Th, ^{235}U, and ^{238}U in cosmochemically Earth-like planets as a function of their age. Owing to its half-life of 14 Gyr, ^{232}Th has declined by only 54% over the age of the Galaxy, while ^{40}K and ^{235}U are effectively extinct and ^{238}U is about 15% of its original concentration. Potassium-40 is abundant relative to the other isotopes, but with a half-life of only 1.25 Gyr, it does not contribute significantly after planets reach ~6 Gyr old.

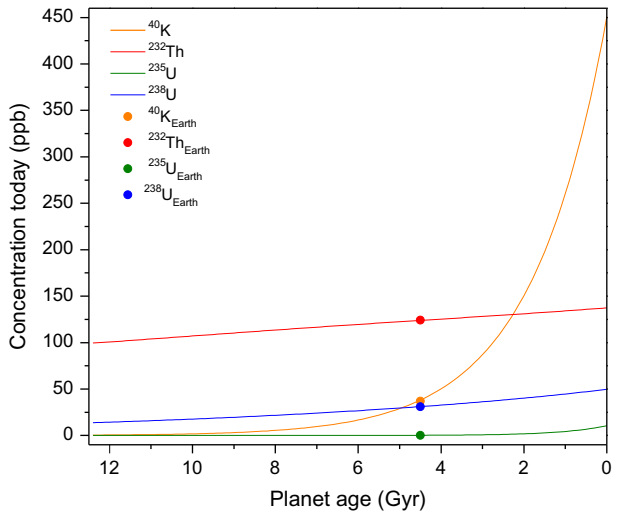

Fig. 9. Concentrations of ^{40}K, ^{232}Th, ^{235}U, and ^{238}U in exoplanets today as a function of their age. The dots show the current concentration of these isotopes in Earth's mantle.

4.5.2. Heating

As expected, young planets are radioactively hotter than old planets. Specifically, as shown in Fig. 10, planets forming today (t_{age} = 0 Gyr) are producing ~8× more heat than an ancient planet which formed at the time the Galaxy formed (t_{age} = 12.5 Gyr). With its relatively short half-life of 704 Myr, ^{235}U does not contribute significantly to heat after ~3 Gyr into a planet's history. The gray band in Fig. 10 shows the end member scenarios for ^{40}K as either only a primary species (minimum) or a secondary species (maximum). The proportions of primary versus secondary contributions turn out to not make a significant difference on the heating outcome. Rather, the age of a planet is a much more important factor. A table of heat production values as a production of age can be found online in Supplementary File S2. We envision that these values can be used in geophysical models of exoplanets.

5. Discussion

5.1. Testing against observations

Similar to the methods of geochronology used for silicate material, long-lived radionuclides can be used to determine the age of stars in nucleocosmochronology. This technique is useful because knowledge of the lifetime of stars is crucial to our understanding of the time scale of stellar processes. Other methods of stellar dating include position in the Hertzsprung–Russell diagram, lithium depletion in clusters via low-mass stars, and asteroseismology (Soderblom, 2010). In contrast to these techniques, nucleocosmochronology is one of the few that is independent of stellar isochrones. However, the technique is hindered by the reliability of heavy element detection due to observational constraints. Presently, robust spectroscopic observations for U and Th are limited to the r-process-enriched, ancient galactic halo stars because they are so metal-poor that there are few absorption line interferences from other elements. With only one weak optical absorption line, Th is the most easily measured long-lived radioactive element. Europium is usually used as a reference element, but its utility has been called into question due to the large difference in atomic mass between it and Th and because these nuclides do not have perfectly identical nucleosynthetic histories (Ludwig et al., 2010). For this reason as well as for the comparable mean half-lives of U and Th relative to Eu, U is considered to be the best element for dating

Table 3
U/Th observations and age estimates of ancient, metal-rich halos stars. Bold values indicate papers that published coupled U/Th data and stellar age predictions.

Object	Reference	log-e(U)	log-e(U) error	log-e(Th)	log-e(Th) error	Ages (Gyr)	(U/Th)	Age error (±Gyr)
BD+17_3248	1	−2	0.1 sigma	−1.18	0.3 sigma	**13.8**	**0.151**	4
	2					12.6		2.6
	2					15.7		3.4
CS22892-052	3	−2.3	N/A	−1.57	±0.1		0.186	
	4	−1.92	N/A	−1.42	0.15 sigma		0.316	
	5	−2.4		−1.6		**16**	**0.158**	4
	6					15.2		3.7
	1					12.8		3
CS30306-132	4	−1.42	N/A	−1.12	0.15 sigma		0.501	
CS31082-001	7	−1.92	N/A	−0.98	±0.05	**14**	**0.115**	2.4
	4	−1.96	N/A	−0.92	0.1 sigma		0.091	
	8	−1.92	±0.11	−0.98	±0.05		0.115	
	9					**12.5**	**0.1821**	3
	2					15		2.6
HD110184	4	−2.52	N/A	−2.5	0.15 sigma		0.955	
HD115444	4	−2.35	N/A	−1.97	0.15 sigma		0.417	
	10	−2.6		−2.23		**14.2**	**0.427**	4
	2					12.4		5.2
HD186478	4	−2	N/A	−1.85	0.15 sigma		0.708	
	11					18.3		4.2
	2					18		3.4
HE0338-3945	12	−0.11	0.38 sigma	0.23	0.17 sigma	**12**	**0.457**	
HE1523-0901	13	−2	N/A	−1.2	N/A	**13.2**	**0.158**	N/A

References: (1) Cowan et al. (2002), (2) Li and Zhao (2009), (3) Sneden et al. (2003), (4) Honda et al. (2004), (5) Sneden et al. (2000), (6) Sneden et al. (1996), (7) Hill et al. (2002), (8) Plez et al. (2004), (9) Cayrel et al. (2001), (10) Westin et al. (2000), (11) Johnson and Bolte (2001), (12) Jonsell et al. (2006), (13) Frebel et al. (2007).

in combination with Th (Clayton, 1988; Ludwig et al., 2010). It is not yet possible to remotely differentiate among isotopes in these astronomical observations, so their elemental ratio (U/Th) must be used in combination with their isotopic production ratio to calculate the age of a star. This is not an issue since all ^{235}U has decayed to extinction in these ancient stars such that ^{238}U is the only uranium isotope that remains.

A way to test our predictions against observations is to take our modeled present-day, age-dependent (U/Th)[3] ratios in Solar Systems and compare them to spectroscopic observations of stars of different ages. The observed (U/Th) ratio in such stars only accounts for ^{238}U and ^{232}Th since we can be confident that ^{235}U is long extinct. The caveats in using these data, however, are that halo stars are among the oldest in the Galaxy, they are unusually enriched in the r-process elements, and they are located far from the solar annulus; all this being said, they are also the only available data with which to test our model. Future observations with more refined techniques will one day provide firmer constraints.

Due to these inherent observational difficulties in studying such weak spectral features as well as the dearth of viable candidates, U was only first measured in a star in 2001. The star CS31982-001 is both extremely metal-poor and enhanced in the r-process elements, making it an ideal candidate for observations. It was originally reported that based on the observed (U/Th), the star has an age of 12.5 ± 3 Gyr (Cayrel et al., 2001). Later observations by separate groups have proposed ages of 14.0 ± 2.4 Gyr (Hill et al., 2002) and 15.5 ± 3.2 Gyr (Schatz et al., 2002). Today, approximately fifteen ancient, metal-poor halo stars have been documented, several more than once, for their U and Th abundances and/or age. Table 3 includes a full list of published data, much of which was accessed through the SAGA database for extremely metal-poor stars (Suda et al., 2008). The mean margin of error of 20% corresponding to about 2.5 Gyr (Ludwig et al., 2010) is carried over to age predictions and reflects the difficulty of these observations and the compelling need for improvements in technique and technology.

Despite the challenges inherent in nucleocosmochronology estimates, we compare the predictions of our model to observations of the ancient halo stars. The problem in this comparison, of course, is that these stars are unlike those located in the solar annulus. They are particularly metal-poor and actinide-enriched, even for halo stars. Indeed, Fig. 11 shows that the observed (U/Th) ratios, with the exception of two stars, are lower than the range predicted from the model though still on the same order of magnitude. The evolving (U/Th) of the model is due to the long half-life of ^{232}Th relative to those of the U isotopes. Should spectroscopic technology improve in the future such that U and Th can be observed in metal-rich stars, we expect that stars in the solar annulus would have comparable (U/Th) ratios as a function of their age with those predicted by our model.

5.2. Heat budgets

An individual planet's thermal evolutionary pathway is dictated in large part by its mass (Stevenson, 1982). In particular, planets need to be large enough to retain internal heat over a long period of time for continued geological activity. Both the Earth's Moon ($0.0123\,M_{\oplus}$) and Mars ($0.107\,M_{\oplus}$) have experienced significant cooling as their accretionary heat dissipated and radiogenic heating failed to sustain vigorous internal convection. Internal heating also maintains a convecting outer core that generates a magnetic field, another potentially important consideration for the long-term maintenance of life on exoplanets. The habitable potential of a planet's surface may be severely suppressed without a magnetic field due to the protection from solar radiation it provides (Dehant et al., 2007). Mars has been observed to have magnetic anomalies, which is suggestive of but not unequivocal evidence for a past magnetic field (Acuña et al., 1998). It may be marginally habitable now in localized environments and almost certainly

[3] The ratio calculations presented here are in the form familiar to geochemists; astronomers instead report abundances of spectroscopic observations as $\log\varepsilon(N_A)$:

$$\log\varepsilon(N_A) = \log\left(\frac{N_A}{N_H}\right) + 12,$$

where N_A and N_H indicate the absolute number densities of a nuclide and hydrogen, respectively, and the equation solves for the difference of the log of their ratios of elemental observations between the star in question and the Sun. We have converted the data reported in this form to absolute ratios, the mathematical derivation of which can be found online in Supplementary File S3.

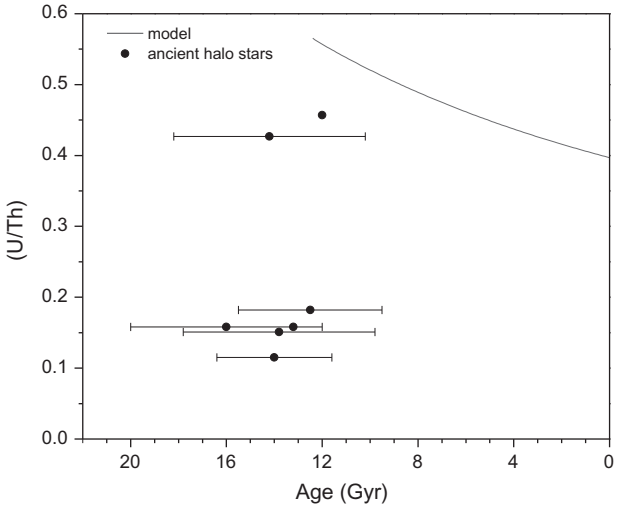

Fig. 11. Modeled (U/Th) ratio compared to the only available stellar U/Th data, which are from ancient metal-poor, actinide-enriched halo stars. The error bars show the wide margin of error on the age estimates. Ratio error bars are not available because errors for U and Th are reported individually (Table 3).

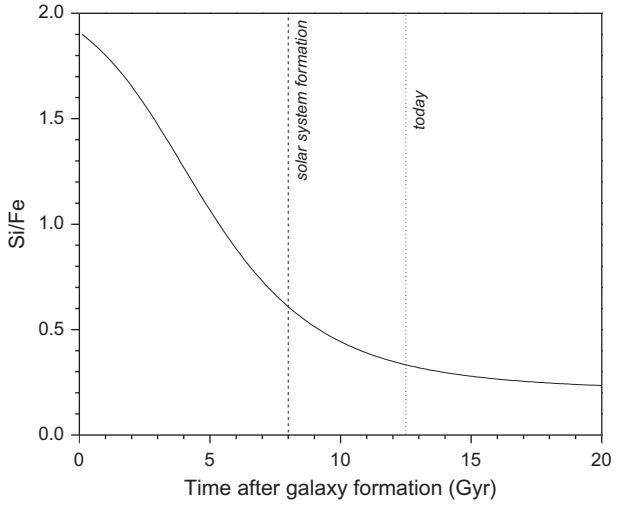

Fig. 12. Si/Fe mass fraction ratio over galactic history. Very early in the Galaxy's history (t < 1 Gyr), the ratio is constant while Si and Fe are both being produced in massive stars, but when Type Ia supernovae begin exploding, the production of Fe increases, resulting in declining Si/Fe.

hosted widespread hospitable environments early in its history (e.g. Nisbet and Sleep, 2001). We consider Mars an adequate lower bound (0.1 $M_\oplus$) for the end-member mass of a habitable planet (i.e. a mini-Earth). For an upper bound, Stevenson (1982) showed that after a protoplanet reaches ~8 $M_\oplus$, its predicted bulk composition quickly transitions from that of a silicate-metal planet to an ice giant like Neptune as nebular gases become gravitationally bound to the rocky core; from this it follows that 8 $M_\oplus$ can be considered a reasonable upper limit for habitable super-Earths. The mass constraints we adopt here for a thermally Earth-like planet are therefore 0.1–8 $M_\oplus$.

A factor tied to nucleosynthesis that will significantly affect a planet's evolution and subsequent capacity to sustain life is iron availability in the young Galaxy (e.g. Gonzalez et al., 2001). This is confirmed by observations of stellar [Fe/H] values (used as an indicator of metallicity) that are found to generally decrease as a function of increasing stellar age (Chiappini et al., 1997). As nucleosynthesis proceeds, the ISM becomes enriched in Fe as it does with U and Th. Because of the delay in Fe nucleosynthesis from Type Ia supernovae, silicate worlds that formed in the early Galaxy might very well have formed with small metal cores, leading to what we term a "super-lunar" planet. This can be quantified by observing how the Si/Fe ratio changes over time (Fig. 12).

A 1-$M_\oplus$ planet with a relatively small lunar-like core (R = 1791 km, R_{core} ~330 km; Weber et al., 2011) will have a correspondingly larger silicate mantle, which means it would have more internal heat than, for example, a 1-$M_\oplus$ planet with a core radius proportional to that of Mercury (R = 2440 km, R_{core} = 2030 km; Smith et al., 2012). Thus, we may postulate that a planet's total heat output will be dictated both by its relative core/mantle size and initial radioactive inventory, in addition to its age. Fig. 13 shows the total heat output for planets of 0.1-, 1-, or 8-$M_\oplus$ and a R_{core}/R ratio like that of the Moon, Earth, or Mercury. The radii corresponding to mass are based on the mass–radius scaling relationship of Seager et al. (2007). A planet of any mass with a core proportional to the Moon's will produce 20% more heat than one of the same mass with an Earth-scale core, and it will produce twice as much as one with a Mercury-scale core. Earth-mass planets of constant radius will produce 8 times more heat than those that are only 0.1 $M_\oplus$; planets that are 8 $M_\oplus$ will produce about 5 times more heat than an Earth-mass planet. Thus, as a result of the galactic [Fe/H] trend, should ancient Solar Systems host planets, we can expect their rocky worlds to have bulk compositions more lunar than Earth- or Mercury-like in their relative metal/silicate abundances. Super-lunar planets may have prevailed in the early Galaxy.

5.3. Planetary evolution and life

Exoplanets that reside in the so-called "habitable zone" of a main-sequence star are of interest due to their potential for having liquid water on their surfaces (Hart, 1979). This property, however, is only a simple first-order evaluation of habitability. Here, we consider habitability to be in the sense of microbial activity. Many other factors must be considered, and since estimating exoplanet habitability is a probability game at best, it is advisable to look for planets that are most similar to Earth. This is why the focus of exoplanet searches, the *Kepler* mission in particular, has been on Earth-mass planets in their star's habitable zone. One cannot definitively state one way or the other whether a particular planet is capable of harboring life, but we can surely argue that planets more similar to Earth than, for example, Mars have a higher likelihood of sustaining environments hospitable to life (as we know it).

An obvious difference between Earth and Mars is the present state of geological activity. This topic is of particular interest because the thermal regime of a planet can dictate its resulting geophysical regime, i.e. mobile-lid convection or stagnant-lid convection (Noack and Breuer, in press). In the case of our own planet, plate tectonics plays a fundamental role in the carbon cycle, helping to keep Earth's surface in thermodynamic disequilibrium (Des Marais, 1994; Parnell, 2004) and its global climate stable via the subduction of seafloor carbonates and subsequent release of CO_2 release back into the atmosphere through volcanism. Both criteria may be necessary for the long-term sustainability of biogeochemical cycles and the emergence of a substantial global-scale biosphere that could modulate atmospheric composition. Microbes can be found nearly everywhere on Earth there exists an exploitable redox gradient, and it is not unreasonable to assume that this would also be necessary for life beyond Earth (Benner et al., 2004). Indeed, there are extremophiles on Earth thriving in environments with a vast array of pH, temperature, pressure, radiation, salinity, desiccation, and chemistry (Rothschild and Mancinelli, 2001). These environments range from deep-sea hydrothermal systems to salty evaporate basins to subglacial lakes, the diversity of which

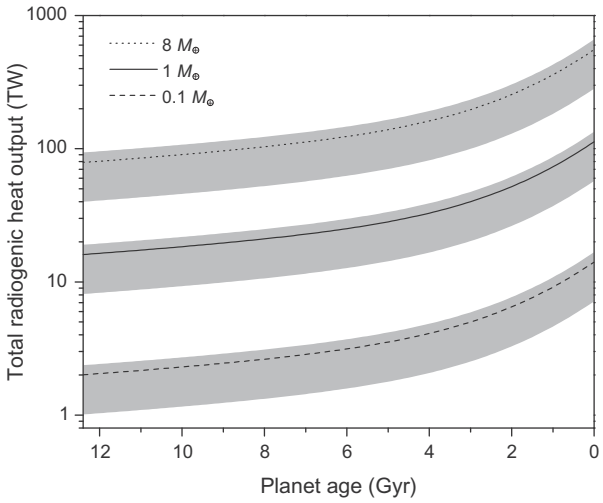

Fig. 13. Total heat output from radiogenic heating as a function of a planet's mass (8, 1, or 0.1 Earth masses), relative core size, and age. The lines show the heat output for planets of different masses that have Earth's mantle/core ratio. The upper and lower bounds of each band are from planets that have the Moon's mantle/core ratio (upper) and Mars' mantle/core ratio (lower).

cannot be provided by a "dead" planet; while other bodies in our Solar System such as Europa (e.g. Chyba and Phillips, 2002), Mars (e.g. McCollom, 2006), and Enceladus (e.g. Parkinson et al., 2008) have been hypothesized to be habitable, microbes on those bodies would have a much narrower selection of relatively hospitable environments from which to choose than that provided by our own geologically active planet. For its role in sustaining life on Earth, it is therefore reasonable to consider the plausibility of plate tectonics as one metric by which the habitable potential of an exoplanet can be judged.

Any scenario that suggests the presence of life on or in a planet requires chemical and physical models for the geochemical and geodynamical origin and evolution of such potentially habitable worlds. As we have shown by coupling a solar system's thermal history with galactic chemical evolution, the degree of radiogenic heat production is dependent on the coupled property of a planet's age and the time at which it formed in galactic history. Radiogenic heat output largely determines the dynamical lifetime and vigor of mantle convection and, by extension, the likelihood that plate tectonics will operate on a rocky planet (Franck, 1998). Of course, there will also be contributions from the heat of accretion and differentiation, and while this cannot be easily quantified in exoplanets, it can only make an exoplanet more likely to be geologically active. If life is in fact dependent upon the presence of plate tectonics, then in the search for extraterrestrial life focus is warranted on those exoplanets that may be thermally similar to Earth.

5.4. Galactic habitable zone

Also important to consider for extrasolar habitability is the concept of a galactic habitable zone (GHZ). This is defined as an annulus in the galactic disk that is sufficiently metal-rich to form rocky planets and has a relatively temperate environment for life to develop, particularly in the context of nearby supernovae rates (e.g. Gonzalez et al., 2001). The GHZ is not just defined in terms of space: time is a key factor as well, given that disk metallicity builds with time, and rocky planets will not form from ISM that is metal-poor. Indeed, a metallicity roughly half of that of the Sun may be required to produce a habitable rocky planet, and the region of the thin disk with sufficient metallicity migrates outwards as the Galaxy ages and becomes enriched in metals via nucleosynthesis (Gonzalez et al., 2001). Lineweaver et al. (2004) evaluated the Milky Way's GHZ in the context of complex multicellular life and estimated that the GHZ annulus corresponds to 7–9 kpc from the galactic center and has stars between 4 and 8 Ga old. Estimates of this annulus width are important given that the chemical and environmental limitations defined by the GHZ preclude Milky Way regions such as the halo, thick disk, outer thin disk, and bulge from having high abundances of hospitable Earth-like planets (Gonzalez et al., 2001). More recent work by Spitoni et al. (2014) involved adding radial gas flows and destructive supernovae processes to evaluations of the GHZ and confirmed the Lineweaver et al. (2004) GHZ annulus estimate of 7–9 kpc. Furthermore, they found that incorporating radial gas flows into the model enhanced the number of stars capable of hosting habitable planets by 38% relative to "classical" GHZ models such as those by Gonzalez et al. (2001) and Lineweaver et al. (2004). This is a promising result as technology for discovering exoplanets and evaluating their habitability continues to be developed.

While the concept of a GHZ is important to take into account in any evaluation of habitability in the Galaxy, in our model, we have restricted the output to an annulus several hundred parsecs in width due to the compositional gradient effects of limited radial mixing (Section 3.2). This is well within the 7–9 kpc annulus proposed by Lineweaver et al. (2004) and confirmed by Spitoni et al. (2014), and our model therefore applies to a region consistent with evaluations of our Galaxy's GHZ.

6. Conclusions

In this work, we have integrated a galactic chemical evolution model with cosmochemical data for our Solar System and geochemical data for the Earth to make age-dependent predictions for radiogenic heating in what we term "cosmochemically Earth-like" exoplanets. By doing so, we have made predictions for both possible bulk compositions and radiogenic heat production rates for rocky exoplanets in the solar annulus. The results show that although young planets start with lower radiogenic heating rates than old planets due to those species being diluted by stable species, the effect of age—and by extension, the period of time that the isotopes have had to decay—overpowers this characteristic. Indeed, exoplanets forming today will have $\sim 7\times$ more heating than a planet that is 12.5 Gyr old, the age of the Galaxy. Those ancient planets may have formed with small cores due to the initially high Si/Fe ratio in the young Galaxy before Type Ia supernovae increased the galactic Fe production rate. This will also have an effect on their total radiogenic heat budgets, as planets with small cores—like the Moon—will have more silicate material, and thus more radiogenic heating, than a planet with a proportionally large core such as Mercury.

While there are many more factors than radiogenic heating that can affect a planet's tectonic regime, radiogenic heating is one that can be constrained. Setting the thermal evolution of an individual planet is important for geophysical models because heat production helps determine both the initial tectonic state of a planet (such as whether plate tectonics is capable of being initiated) and its subsequent evolution. We envision that the heat productions predicted here will be incorporated into geophysical models of exoplanets. This is imperative because a geologically active exoplanet, in the context of the search for Earth-like planets, is more likely to be capable of supporting life on a global scale than a dead planet. Fig. 14 shows the predicted heat production rates for cosmochemically Earth-like planets as a function of their age superimposed with the age distribution for dated stars with confirmed exoplanets, both gaseous and rocky, as of 2012. The peak of ages around that of the Sun is a selection bias towards stars that were

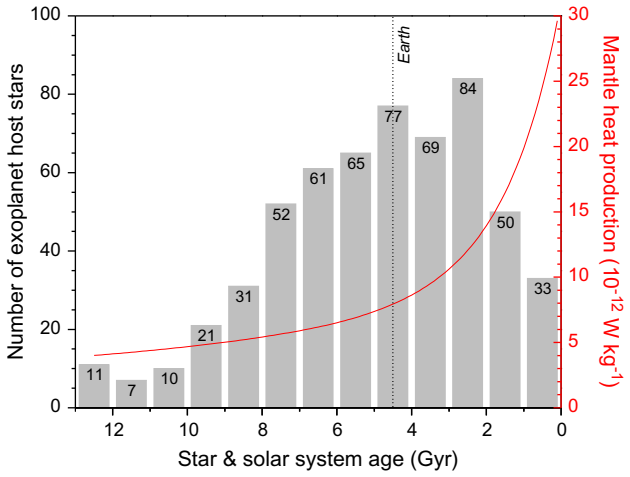

Fig. 14. Number of exoplanet host stars as a function of their age in 2012 superimposed with the predicted current heat production for cosmochemically Earth-like planets. The host stars include those that have either gaseous or rocky planets, and some stars are known to host multiple planets.

chosen for detailed observation due to their Sun-like qualities. The salient point from this figure is that in the search for Earth-like exoplanets, as previously considered by other workers, stars within a couple billion years in age from that of the Sun are most promising for their abilities to host life (e.g. Lineweaver et al., 2004; Spitoni et al., 2014). Rocky planets in these solar systems might be old enough to be beyond the period of late accretion but young enough such that their internal heat product is still sufficient for geological activity that may be expressed in the form of plate tectonics. Hotter planets are more likely to be geologically active, so future searches for exoplanet host stars should be directed towards young stars that might host planets that are Earth-like in terms of their chemistry in addition to their size and orbital parameters.

Acknowledgments

We have benefited from debates and discussions with E. Bergin, G. Blake, N. Coltice, J. Cowan, N. Dauphas, C. Lineweaver, L. Nittler, L. Noack, H. Rauer, D. Stevenson, and W.H. Waller. E.A.F. acknowledges support from the NASA Earth and Space Sciences Fellowship Program (NNX11AR74H) and the Amelia Earhart Fellowship awarded by Zonta International. S.J.M. acknowledges NASA Exobiology Grant No. NNX10AH78G and the NASA Lunar Science Institute (A99168JD through the Center for Lunar Origin and Evolution, CLOE) for support of this work. Additional support to S.J.M. came from the Lyon Institut des Origines and a Visiting Distinguished Professorship at the Hungarian Academy of Sciences, Research Center for Astronomy and Earth Sciences. Comments by three anonymous reviewers and editorial handling by G. Tinetti helped to improve the manuscript.

Appendix A. Supplementary material

Supplementary data associated with this article can be found, in the online version, at http://dx.doi.org/10.1016/j.icarus.2014.08.031.

References

Acuña, M.H. et al., 1998. Magnetic field and plasma observations at Mars: Initial results of the Mars Global Surveyor mission. Science 279 (80), 1676–1680. http://dx.doi.org/10.1126/science.279.5357.1676.

Amelin, Y., Krot, A.N., Hutcheon, I.D., Ulyanov, A.A., 2002. Lead isotopic ages of chondrules and calcium–aluminum-rich inclusions. Science 297 (80), 1678–1683. http://dx.doi.org/10.1126/science.1073950.

Anders, E., Grevesse, N., 1989. Abundances of the elements – Meteoritic and solar. Geochim. Cosmochim. Acta 53, 197–214.

Barclay, T. et al., 2013. A sub-Mercury-sized exoplanet. Nature 494, 452–454. http://dx.doi.org/10.1038/nature11914.

Benner, S.A., Ricardo, A., Carrigan, M.A., 2004. Is there a common chemical model for life in the Universe? Curr. Opin. Chem. Biol. 8, 672–689. http://dx.doi.org/10.1016/j.cbpa.2004.10.003.

Bensby, T., Feltzing, S., Lundströsm, I., 2004. A possible age-metallicity relation in the galactic thick disk? Astron. Astrophys. 421, 969–976. http://dx.doi.org/10.1051/0004-6361:20035957.

Boeche, C. et al., 2013. The relation between chemical abundances and kinematics of the galactic disc with RAVE. Astron. Astrophys. 553, A19. http://dx.doi.org/10.1051/0004-6361/201219607.

Boissier, S., Prantzos, N., 1999. Chemo-spectrophotometric evolution of spiral galaxies – I. The model and the Milky Way. Mon. Not. R. Astron. Soc. 307, 857–876. http://dx.doi.org/10.1046/j.1365-8711.1999.02699.x.

Bond, J.C., Lauretta, D.S., O'Brien, D.P., 2010. Making the Earth: Combining dynamics and chemistry in the Solar System. Icarus 205, 321–337. http://dx.doi.org/10.1016/j.icarus.2009.07.037.

Bouvier, A., Wadhwa, M., 2010. The age of the Solar System redefined by the oldest Pb–Pb age of a meteoritic inclusion. Nat. Geosci. 3, 637–641. http://dx.doi.org/10.1038/ngeo941.

Bromm, V., Larson, R.B., 2004. The first stars. Annu. Rev. Astron. Astrophys. 42, 79–118. http://dx.doi.org/10.1146/annurev.astro.42.053102.134034.

Burbidge, E., Burbidge, G., Fowler, W., Hoyle, F., 1957. Synthesis of the elements in stars. Rev. Mod. Phys. 29, 547–650. http://dx.doi.org/10.1103/RevModPhys.29.547.

Canup, R., 2008. Lunar-forming collisions with pre-impact rotation. Icarus 196, 518–538. http://dx.doi.org/10.1016/j.icarus.2008.03.011.

Caro, G., 2011. Early silicate Earth differentiation. Annu. Rev. Earth Planet. Sci. 39, 31–58. http://dx.doi.org/10.1146/annurev-earth-040610-133400.

Cayrel, R. et al., 2001. Measurement of stellar age from uranium decay. Nature 409, 691–692. http://dx.doi.org/10.1038/35055507.

Chiappini, C., Matteucci, F., Gratton, R., 1997. The chemical evolution of the Galaxy: The two-infall model. Astrophys. J. 477, 765–780. http://dx.doi.org/10.1086/303726.

Chou, C.-L., 1978. Fractionation of siderophile elements in the Earth's upper mantle. Proc. Lunar Sci. Conf. 9.

Chyba, C., Phillips, C., 2002. Europa as an abode for life. Orig. Life Evol. Biosph. 6, 3–16.

Clayton, D.D., 1985. Galactic chemical evolution and nucleocosmochronology: A standard model. In: Arnett, W.D., Truran, J.W. (Eds.), Nucleosynthesis: Challenges and New Developments. University of Chicago Press, Chicago, p. 65.

Clayton, D.D., 1988. Nuclear cosmochronology within analytic models of the chemical evolution of the solar neighbourhood. Mon. Not. R. Astron. Soc. 234, 1–36.

Clayton, D.D., 2003. Handbook of Isotopes in the Cosmos. Cambridge University Press, Cambridge.

Cowan, J.J., Sneden, C., 2006. Heavy element synthesis in the oldest stars and the early Universe. Nature 440, 1151–1156. http://dx.doi.org/10.1038/nature04807.

Cowan, J.J., Thielemann, F.K., Truran, J.W., 1991. Radioactive dating of the elements. Annu. Rev. Astron. Astrophys. 29, 447–497. http://dx.doi.org/10.1146/annurev.aa.29.090191.002311.

Cowan, J.J. et al., 2002. The chemical composition and age of the metal-poor halo star BD +17∗3248. Astrophys. J. 572, 861–879.

Dauphas, N., 2005. The U/Th production ratio and the age of the Milky Way from meteorites and galactic halo stars. Nature 435, 1203–1205. http://dx.doi.org/10.1038/nature03645.

De Avillez, M.A., Mac Low, M., 2002. Mixing timescales in a supernova-driven interstellar medium. Astrophys. J. 581, 1047–1060. http://dx.doi.org/10.1086/344256.

Dehant, V. et al., 2007. Planetary magnetic dynamo effect on atmospheric protection of early Earth and Mars. Space Sci. Rev. 129, 279–300. http://dx.doi.org/10.1007/s11214-007-9163-9 (Space Sciences Series of ISSI).

Des Marais, D.J., 1994. Tectonic control of the crustal organic carbon reservoir during the Precambrian. Chem. Geol. 114, 303–314. http://dx.doi.org/10.1016/0009-2541(94)90060-4.

Finkelstein, S.L. et al., 2013. A Galaxy rapidly forming stars 700 million years after the Big Bang at redshift 7.51. Nature 502, 524–527. http://dx.doi.org/10.1038/nature12657.

Foley, B.J., Bercovici, D., Landuyt, W., 2012. The conditions for plate tectonics on super-Earths: Inferences from convection models with damage. Earth Planet. Sci. Lett. 331–332, 281–290. http://dx.doi.org/10.1016/j.epsl.2012.03.028.

Fortney, J.J., Marley, M.S., Barnes, J.W., 2007. Planetary radii across five orders of magnitude in mass and stellar insolation: Application to transits. Astrophys. J., 1661–1672.

Franck, S., 1998. Evolution of the global mean heat flow over 4.6 Gyr. Tectonophysics 291, 9–18.

Frebel, A., Christlieb, N., Norris, J.E., Thom, C., Beers, T.C., Rhee, J., 2007. Discovery of HE 1523-0901, a strongly r-process-enhanced metal-poor star with detected uranium. Astrophys. J. 660, L117–L120. http://dx.doi.org/10.1086/518122.

Goldschmidt, V.M., 1954. Geochemistry. Clarendon Press, Oxford.

Gomes, R., Levison, H.F., Tsiganis, K., Morbidelli, a., 2005. Origin of the cataclysmic Late Heavy Bombardment period of the terrestrial planets. Nature 435, 466–469. http://dx.doi.org/10.1038/nature03676.

Gonzalez, G., Brownlee, D., Ward, P., 2001. The galactic habitable zone: Galactic chemical evolution. Icarus 152, 185–200. http://dx.doi.org/10.1006/icar.2001.6617.

Hart, M.H., 1979. Habitable zones about main sequence stars. Icarus 37, 351–357. http://dx.doi.org/10.1016/0019-1035(79)90141-6.

Hill, V. et al., 2002. First stars. I: The extreme r-element rich, iron-poor halo giant CS 31082-001 – Implications for the r-process site(s) and radioactive cosmochronology. Astron. Astrophys. 387, 560–579. http://dx.doi.org/10.1051/0004-6361.

Hillebrandt, W., Niemeyer, J.C., 2000. Type Ia supernova explosion models. Annu. Rev. Astron. Astrophys. 38, 191–230. http://dx.doi.org/10.1146/annurev.astro.38.1.191.

Honda, S. et al., 2004. Spectroscopic studies of extremely metal-poor stars with the subaru high dispersion. Astrophys. J., 474–498.

Huss, G.R., Meyer, B.S., Srinivasan, G., Goswami, J.N., Sahijpal, S., 2009. Stellar sources of the short-lived radionuclides in the early Solar System. Geochim. Cosmochim. Acta 73, 4922–4945. http://dx.doi.org/10.1016/j.gca.2009.01.039.

Johnson, J.A., Bolte, M., 2001. Th ages for metal-poor stars. Astrophys. J. 20, 888–902.

Johnson, J.A., Winn, J.N., Albrecht, S., Howard, A.W., Marcy, G.W., Gazak, J.Z., 2009. A third exoplanetary system with misaligned orbital and stellar spin axes. Publ. Astron. Soc. Pacific 121, 1104–1111. http://dx.doi.org/10.1086/644604.

Jonsell, K. et al., 2006. The Hamburg/ESO R-process enhanced star survey (HERES) III. HE 0338-3945 and the formation of the r + s stars. Astron. Astrophys. 670, 651–670. http://dx.doi.org/10.1051/0004-6361.

Kargel, J.S., Lewis, J.S., 1993. The composition and early evolution of Earth. Icarus 105, 1–25. http://dx.doi.org/10.1006/icar.1993.1108.

Kite, E.S., Manga, M., Gaidos, E., 2009. Geodynamics and rate of volcanism on massive Earth-like planets. Astrophys. J. 700, 1732–1749. http://dx.doi.org/10.1088/0004-637X/700/2/1732.

Lenardic, A., Cooper, C.M., Moresi, L., 2011. A note on continents and the Earth's Urey ratio. Phys. Earth Planet. Inter. 188, 127–130. http://dx.doi.org/10.1016/j.pepi.2011.06.008.

Li, J., Zhao, G., 2009. Radioactive ages of metal-poor halo stars. Chin. J. Astron. Astrophys. 75, 75–87.

Lineweaver, C.H., Fenner, Y., Gibson, B.K., 2004. The galactic habitable zone and the age distribution of complex life in the Milky Way. Science 303 (80), 59–62. http://dx.doi.org/10.1126/science.1092322.

Lodders, K., 2003. Solar System abundances and condensation temperatures of the elements. Astrophys. J. 591, 1220–1247. http://dx.doi.org/10.1086/375492.

Ludwig, H.-G., Caffau, E., Steffen, M., Bonifacio, P., Sbordone, L., 2010. Accuracy of spectroscopy-based radioactive dating of stars. Astron. Astrophys. 509, A84. http://dx.doi.org/10.1051/0004-6361/200810780.

Madau, P., Pozzetti, L., Dickinson, M., 1998. The star formation history of field galaxies. Astrophys. J. 498, 106–116. http://dx.doi.org/10.1086/305523.

Matteucci, F., 2003. The Chemical Evolution of the Galaxy. Kluwer Academic Publishers, Dordrecht, The Netherlands.

Matteucci, F., Greggio, L., 1986. Relative roles of type I and II supernovae in the chemical enrichment of the interstellar gas. Astron. Astrophys. 154, 279–287.

Mayor, M., Queloz, D., 1995. A Jupiter-mass companion to a solar-type star. Nature 378, 355–359. http://dx.doi.org/10.1038/378355a0.

McCollom, T.M., 2006. The habitability of Mars: Past and present. In: Blondel, P., Mason, J.W. (Eds.), Solar System Update. Springer-Verlag, Berlin, pp. 159–175. http://dx.doi.org/10.1007/3-540-37683-6_6.

McDonough, W., Sun, S., 1995. The composition of the Earth. Chem. Geol. 2541, 223–253.

Mihalas, D., Binney, J., 1981. Galactic Astronomy: Structure and Kinematics, second ed. W.H. Freeman & Co., San Francisco.

Nisbet, E.G., Sleep, N.H., 2001. The habitat and nature of early life. Nature 409, 1083–1091. http://dx.doi.org/10.1038/35059210.

Nittler, L.R., Dauphas, N., 2006. Meteorites and the chemical evolution of the Milky Way. In: Lauretta, D.S., McSween, H.Y., Jr. (Eds.), Meteorites and the Early Solar System II. University of Arizona Press, Tucson, pp. 127–146.

Noack, L., Breuer, D., in press. Plate tectonics on rocky exoplanets: Influence of initial conditions and mantle rheology. Planet. Space Sci. http://dx.doi.org/10.1016/j.pss.2013.06.020.

O'Neill, C.J., 2012. Tectonothermal evolution of solid bodies: Terrestrial planets, exoplanets and moons. Aust. J. Earth Sci. 59, 189–198. http://dx.doi.org/10.1080/08120099.2012.644403.

Pagel, B.E.J., 1997. Nucleosynthesis and Chemical Evolution of Galaxies. Cambridge University Press, Cambridge.

Papuc, A.M., Davies, G.F., 2008. The internal activity and thermal evolution of Earth-like planets. Icarus 195, 447–458. http://dx.doi.org/10.1016/j.icarus.2007.12.016.

Parkinson, C.D., Liang, M.-C., Yung, Y.L., Kirschivnk, J.L., 2008. Habitability of Enceladus: Planetary conditions for life. Orig. Life Evol. Biosph. 38, 355–369. http://dx.doi.org/10.1007/s11084-008-9135-4.

Parnell, J., 2004. Plate tectonics, surface mineralogy, and the early evolution of life. Int. J. Astrobiol. 3, 131–137. http://dx.doi.org/10.1017/S1473550404002101.

Plez, B. et al., 2004. Lead abundance in the uranium star CS 31082-001. Astron. Astrophys. 12, 9–12. http://dx.doi.org/10.1051/0004-6361.

Reeves, H., 1991. Nucleochronology revisited. Astron. Astrophys. 244, 294–297.

Richter, F.M., 1988. A major change in the thermal state of the Earth at the Archean–Proterozoic boundary: Consequences for the nature and preservation of continental lithosphere. J. Petrol., 39–52. http://dx.doi.org/10.1093/petrology/Special_Volume. 1.39.

Rothschild, L.J., Mancinelli, R.L., 2001. Life in extreme environments. Nature 409, 1092–1101.

Schatz, H. et al., 2002. Thorium and uranium chronometers applied to CS 31082-001. Astrophys. J. 579, 626–638. http://dx.doi.org/10.1086/342939.

Seager, S., Kuchner, M., Hier-Majumder, C.A., Militzer, B., 2007. Mass–radius relationships for solid exoplanets. Astrophys. J. 669, 1279–1297. http://dx.doi.org/10.1086/521346.

Sleep, N.H., 2007. Plate tectonics through time. Treatise Geophys. 9, 145–169. http://dx.doi.org/10.1016/B978-044452748-6.00143-7.

Smith, D.E. et al., 2012. Gravity field and internal structure of Mercury from MESSENGER. Science 336 (80), 214–217. http://dx.doi.org/10.1126/science.1218809.

Sneden, C., McWilliam, A., Preston, G.W., Cowan, J.J., Burris, D.L., Armosky, B.J., 1996. The ultra-metal-poor, neutron-capture-rich giant star CS 22892-052. Astrophys. J. 467, 819. http://dx.doi.org/10.1086/177656.

Sneden, C. et al., 2000. Evidence of multiple r-process sites in the early Galaxy: New observations of CS 22892-052. Astrophys. J. 533, L139–L142. http://dx.doi.org/10.1086/312631.

Sneden, C. et al., 2003. The extremely metal-poor, neutron capture-rich Star CS 22892-052: A comprehensive abundance analysis. Astrophys. J. 591, 936–953. http://dx.doi.org/10.1086/375491.

Sneden, C., Cowan, J.J., Gallino, R., 2008. Neutron-capture elements in the early Galaxy. Annu. Rev. Astron. Astrophys. 46, 241–288. http://dx.doi.org/10.1146/annurev.astro.46.060407.145207.

Soderblom, D.R., 2010. The ages of stars. Annu. Rev. Astron. Astrophys. 48, 581–629. http://dx.doi.org/10.1146/annurev-astro-081309-130806.

Spitoni, E., Matteucci, F., Sozzetti, A., 2014. The galactic habitable zone of the Milky Way and M31 from chemical evolution models with gas radial flows. Mon. Not. R. Astron. Soc. 440, 2588–2598. http://dx.doi.org/10.1093/mnras/stu484.

Stevenson, D.J., 1982. Formation of the giant planets. Planet. Space Sci. 30, 755–764. http://dx.doi.org/10.1016/0032-0633(82)90108-8.

Suda, T. et al., 2008. Stellar Abundances for the Galactic Archeology (SAGA) Database—Compilation of the Characteristics of Known Extremely Metal-Poor Stars. Publ. Astron. Soc., Japan.

Tinsley, B.M., 1979. Stellar lifetimes and abundance ratios in chemical evolution. Astrophys. J. 229, 1046–1056. http://dx.doi.org/10.1086/157039.

Turcotte, D.L., Schubert, G., 2002. Geodynamics, second ed. Cambridge University Press, New York.

Valencia, D., O'Connell, R.J., 2009. Convection scaling and subduction on Earth and super-Earths. Earth Planet. Sci. Lett. 286, 492–502. http://dx.doi.org/10.1016/j.epsl.2009.07.015.

Valencia, D., O'Connell, R.J., Sasselov, D., 2006. Internal structure of massive terrestrial planets. Icarus 181, 545–554. http://dx.doi.org/10.1016/j.icarus.2005.11.021.

Valencia, D., O'Connell, R.J., Sasselov, D.D., 2007. Inevitability of plate tectonics on super-Earths. Astrophys. J. 670, L45–L48. http://dx.doi.org/10.1086/524012.

Wasserburg, G.J., Busso, M., Gallino, R., 1996. Abundances of actinides and short-lived nonactinides in the interstellar medium: Diverse supernova sources for the r-processes. Astrophys. J. 466, L109–L113. http://dx.doi.org/10.1086/310177.

Weber, R.C., Lin, P.-Y., Garnero, E.J., Williams, Q., Lognonné, P., 2011. Seismic detection of the lunar core. Science 331 (80), 309–312. http://dx.doi.org/10.1126/science.1199375.

Westin, J., Sneden, C., Gustafsson, B., Cowan, J.J., 2000. The r-process-enriched low-metallicity giant HD 115444. Astrophys. J. 530, 783–799. http://dx.doi.org/10.1086/308407.

Zhang, H.W., Gehren, T., Butler, K., Shi, J.R., Zhao, G., 2006. Potassium abundances in nearby metal-poor stars. Astron. Astrophys. 457, 645–650. http://dx.doi.org/10.1051/0004-6361:20064909.